

# Finite Element Modeling for the Mechanical Behavior of Silicon Diaphragms Using Comsol Multiphysics

J. Ren<sup>\*1</sup>, M. Ward<sup>1</sup>

<sup>1</sup>School of Mechanical Engineering, the University of Birmingham, UK

Peter Kinnell<sup>2</sup>, Russell Cradock<sup>2</sup>

<sup>2</sup>GE Druck Limited, Fir Tree Lane, Leicester, UK

\*Corresponding author: Edgbaston, Birmingham, B15 2TT, jxr551@bham.ac.uk

**Abstract:** The silicon diaphragm is one of the most common structures in micro-electro-mechanical systems (MEMS). However, it is susceptible to creep deformation at elevated temperatures. This paper presents a transient finite element model which simulates the mechanical behavior of the micromachined silicon diaphragms at the temperature of 1173K (900°C). The constitutive equations proposed by Alexander and Hassen are employed in Comsol Multiphysics. The results show that the larger the diaphragm radius, the larger the density of the moving dislocation is. There is good agreement between the model prediction and the experiment data for the diaphragms with a radius in the range of 1.5mm to 2mm. However, the model is not valid for the diaphragm with a radius of 2.5mm. This is because the generated dislocation density is very high and slip resistance is not included in present model.

**Keywords:** MEMS, silicon diaphragms, creep, constitutive model, FEA modeling

## 1. Introduction

Silicon diaphragms are one of the most common structures in micro-electro-mechanical systems (MEMS) [1]. For micromachined pressure sensors, the silicon diaphragms are widely used as sensing element to detect the magnitude of external pressure. Since high temperature pressure sensors are required for industrial, automotive and aerospace sensing applications, the load-deflection behavior of the silicon diaphragm at elevated temperatures is studied by experiment and is modeled using Comsol Multiphysics.

Single crystal silicon is brittle at low temperatures, but at temperatures higher than 550°C, the motion of the dislocations under an applied stress is thermally activated, thus silicon becomes ductile material [2]. Therefore, silicon

diaphragms which are intended to sensing pressure at elevated temperature may suffer from plastic deformation (creep). Wherever applied stress exceeds the critical resolved shear stress (CRSS), the crystallographic slip of the dislocations occurs. The slip systems of silicon are along  $\langle 011 \rangle$  directions on the dense atomic planes  $\{111\}$ . The number of dislocations increases rapidly due to Frank-Read source. Because of their low dislocation density, the dislocations do not interact with each others motion. It has been proposed that the magnitude of the plastic shear strain rate is governed by the dislocation density in the initial stage of the deformation by the Alexander and Hassen's model [3]. After a large number of dislocations have been generated, the interaction of dislocations resists to the plastic flow. As a result, it is proposed that the slip resistance governs the plastic strain rate in the later stage of the deformation [4].

The constitutive model proposed by Alexander and Hassen is universally used for the study of the elevated temperature behavior of silicon and other semiconductors [5] [6] [7]. The model uses coupled equations to describe the evolution of the dislocation density. The plastic strain rate and dislocation multiplication are related to the temperature and the applied stress. The model has been proved to be valid over a stress range of 10MPa to 120MPa and a temperature range of 900K to 1200K [5].

This work presented here is focused on the elevated temperature behavior of the silicon diaphragm in the initial deformation stage. First, the experiment to characterize the deformation of micromachined silicon diaphragms is presented. Second, the basic constitutive equations used in the Alexander and Hassen's model are briefly recalled. The transient finite element model built in COMSOL Multiphysics is then described including the material parameters. In section 4,

the dislocation density is investigated using the model as a function of the diaphragm radius. The predicted diaphragm deformations are compared with experimental results. The strengths and the limitations of the present model are discussed in the conclusion section.

## 2. Experimental procedure

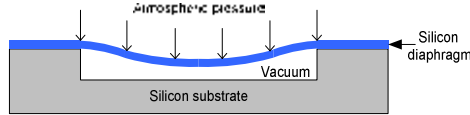


**Figure 1.** Schematic of cross-sectional view of the test sample.

The schematic of the sample is shown in figure 1. The silicon diaphragm is clamped to the silicon substrate. Because the cavity is sealed in vacuum, the diaphragm deflects toward substrate under atmospheric pressure. The thickness of the diaphragm is 50  $\mu\text{m}$ . The size of the silicon diaphragms is determined by the radius of the cavity which is in the range of 1.5mm to 2.5mm.

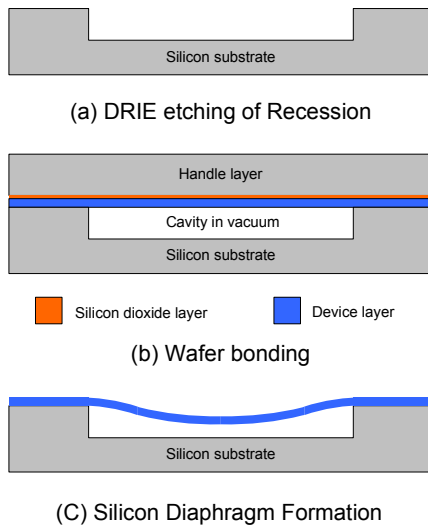


**Figure 2** Process flow of the test sample

The test samples were manufactured using MEMS technology. The fabrication process is shown in figure 2. The silicon wafers are (100) oriented and are doped with boron. In order to form the cavity, a prime silicon wafer was first etched by deep reactive ion etching, as shown in figure 2 (a). Then the prime silicon wafer was bonded with a BESOI wafer using silicon fusion

wafer bonding. Figure 2 (b) shows the schematic after wafer bonding. The test samples were made after the handle layer and the silicon dioxide layer of the BESOI wafer were removed by using KOH and HF wet etching separately, as illustrated in figure 2 (c).

The surface profiles of the test sample under atmospheric pressure were measured using a white light interferometer. Then the samples were subjected to annealing in a tube furnace. As illustrated in figure 3, the furnace temperature rose from 873K (600°C) to 1173K (900°C) with the ramp-up rate of temperature 5K/min (5°C/min). Then the annealing temperature was maintained at 1173K (900°C) for 1 hour. After that, the furnace was cooled down gradually to 873K (600°C) with the ramp-down rate of temperature -5K/min (-5°C/min). In order to induce stress for creep, nitrogen gas at atmospheric pressure was applied during annealing. After annealing, the surface profiles were measured again under atmospheric pressure at room temperature.

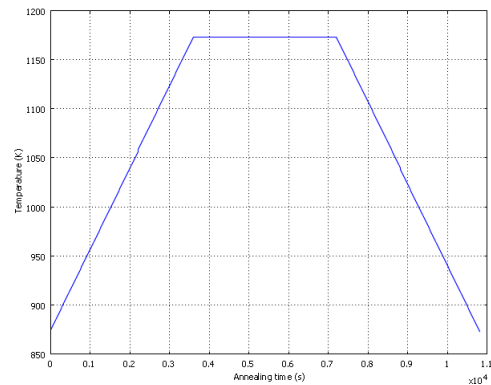


**Figure 3.** Furnace temperature as a function of time

## 3. Constitutive equations

Alexander and Hassen's model (AH model) assumes that the distribution of the dislocation is initially uniform in the whole sample [3]. The plastic shear strain rate, which is related to the motion of the mobile dislocations, can be expressed as:

$$\dot{\gamma}^p = \rho b v_0 \exp(-Q/kT) \left( \frac{\tau_{eff}}{\tau_0} \right)^{1/m} \text{sign}(\tau_{eff}) \quad (1)$$

where  $\rho$  is the dislocation density,  $b$  is the Burgers vector magnitude,  $v_0$  is a reference value for dislocation velocity,  $Q$  is the an activation energy,  $k$  is the Boltzmann constant,  $T$  is the absolute temperature in Kelvin,  $\tau_0$  is a reference stress,  $m$  is a strain rate hardening exponent, and  $\tau_{eff}$  is the effective stress given by:

$$\tau_{eff} = \tau - \alpha \mu b \sqrt{\rho} \quad (2)$$

where  $\tau$  is the equivalent shear stress,  $\alpha$  is a constant and  $\mu$  is a shear modulus. The second term at the right hand side of equation (2) represents the internal stress produced by the interaction of the dislocations.

The evolution equation for the dislocation density is given by:

$$\dot{\rho} = \left( \frac{K}{b} \right) \dot{\gamma}^p \tau_{eff} \quad (3)$$

where  $K$  is a multiplication rate constant. The dislocation multiplication rate is related to the magnitude of the plastic strain rate and the effective stress.

The viscoplastic strain rate tensor is proportional to the shear strain rate.

$$\dot{\epsilon}_{ij}^{vp} = \frac{3}{2} \dot{\gamma}^p \frac{S_{ij}}{\sigma_e} \quad (4)$$

where  $\sigma_e$  is the von Mises effective stress,  $S_{ij}$  is the deviatoric stress tensor. The viscoplastic strain rate tensor for two dimensional axisymmetrical problem can be expressed as:

$$(\dot{\epsilon}^{vp})_r = \frac{3}{2} \dot{\gamma}^p \frac{(2\sigma_r - \sigma_\phi - \sigma_z)}{3\sigma_e} \quad (5a)$$

$$(\dot{\epsilon}^{vp})_\phi = \frac{3}{2} \dot{\gamma}^p \frac{(2\sigma_\phi - \sigma_r - \sigma_z)}{3\sigma_e} \quad (5b)$$

$$(\dot{\epsilon}^{vp})_z = \frac{3}{2} \dot{\gamma}^p \frac{(2\sigma_z - \sigma_r - \sigma_\phi)}{3\sigma_e} \quad (5c)$$

$$(\dot{\epsilon}^{vp})_{rz} = \frac{3}{2} \dot{\gamma}^p \frac{\sigma_{rz}}{\sigma_e} \quad (5d)$$

The total strain rate is given by

$$\dot{\epsilon}_{ij} = \dot{\epsilon}_{ij}^{el} + \dot{\epsilon}_{ij}^{vp} + \dot{\epsilon}_{ij}^{th} \quad (6)$$

where  $\dot{\epsilon}_{ij}^{el}$  is the elastic strain rate and  $\dot{\epsilon}_{ij}^{th}$  is the thermal strain rate.

#### 4. Use of COMSOL Multiphysics

The model simulates the displacement field of the silicon diaphragm using Stress-Strain application mode of MEMS Module in axial symmetry (2D). Figure 4 shows the schematic drawing. The atmospheric pressure is applied on the top of the silicon diaphragm. When calculating the elastic deformation, the boundaries of the silicon substrate are considered as fixed boundaries. However, the sample is free to expand in the furnace during annealing. As a result, the stress due to thermal expansion is ignored in the model. Silicon is anisotropic material which has an orientation-dependent modulus of elasticity. The equivalent values for (100) orientated silicon are applied. The Young's modulus and Poisson's ratio are set to 151 GPa and 0.1615, separately [8].

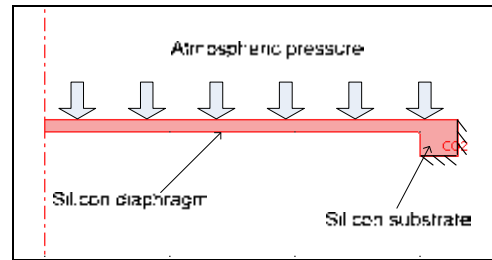


**Figure 4.** Schematic drawing of the silicon diaphragm with fixed edge

The plastic strain rate and the effective stress are defined in the scalar expressions. The Burger's vector  $b$  is  $3.83 \times 10^{-10}$  m. The activation energy  $Q$  is  $3.47 \times 10^{-19}$  J. Parameter  $m$  is 0.9. The dislocation velocity for boron doped silicon is only slightly smaller than that in high purity silicon. The magnitude of the reference dislocation velocity is  $6.0 \times 10^3$  m/s for 60 °C dislocations and is  $7.0 \times 10^3$  m/s for screw dislocations under a shear stress of 20 MPa [9]. Therefore, an average value of  $6.5 \times 10^3$  m/s is used for  $v_0$ . Equation 1 holds only when the effective stress  $\tau_{eff}$  is positive. Therefore,  $\tau_{eff}$  is obtained at the region where  $\tau > \alpha \mu b$ . The constant  $\alpha$  is 2. The shear modulus  $\mu$  is 64 GPa.

Two PDE general form modes are used to compute the dislocation density  $\rho$  and the viscoplastic strain  $\epsilon^{vp}$ . There are a few grown-in dislocations in single crystal silicon. The initial dislocation density  $\rho_0$  is estimated as  $2 \times 10^7 / \text{m}^2$ .

The evolution of dislocation density with time is mainly controlled by the multiplication rate constant  $K$ . The PDE modes are coupled to the Stress-Strain application mode. According to equation (6), the viscoplastic strains should be excluded from the total strains in the expressions for the elastic stresses of equation system. Then the displacement obtained from the Stress-Strain application mode represents both plastic and elastic deformation.

## 5. Results and Discussion

### 5.1 Dislocation density

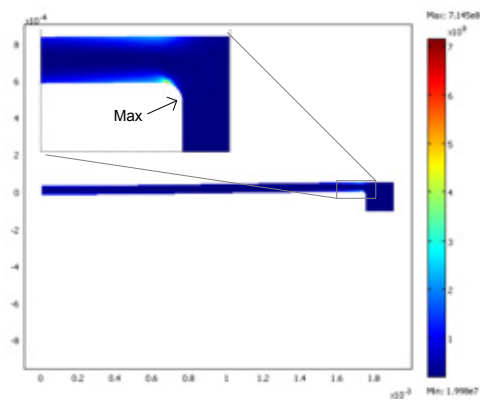


**Figure 5.** The dislocation density distribution after annealing (radius=1.75mm)

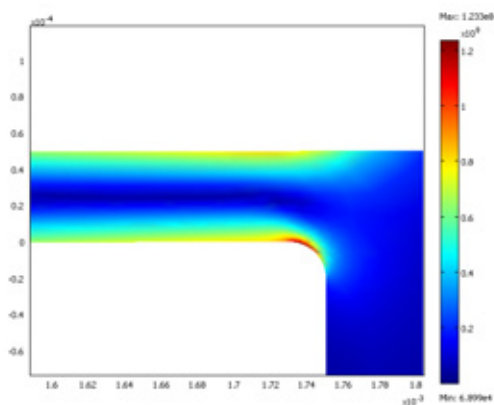
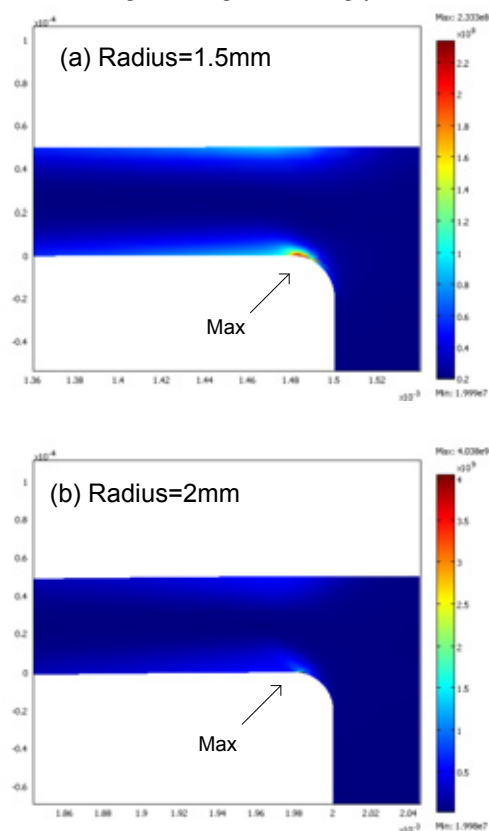


**Figure 6.** Von Mises effective stress of the diaphragm under the atmospheric pressure before annealing (radius=1.75mm)

The density of moving dislocations influences the mechanical behaviour of silicon. Figure 5 predicts the distribution of the dislocation density in the silicon diaphragm with a radius of 1.75mm after annealing. The

dislocation multiplication rate is very low at the region close to the middle plane of the diaphragm. The dislocation densities of about  $3 \times 10^8/\text{m}^2$  are found at the upper and lower surface near the diaphragm edge as illustrated by the light blue color in the figure. The maximum dislocation densities of about  $7.15 \times 10^8/\text{m}^2$  are concentrated in a small region at the lower corner near the edge of the diaphragm. This results from the stress concentration at the round corner, as shown in figure 6. The maximum von Mises effective stress in the small region is 123MPa. This value is much higher than that of about 80MPa in the region nearby.

Using the same initial settings, the model was run for various diaphragm semidiameter. The dislocation density distributions near the diaphragm edge are shown in figure 7. The results indicate that the larger the diaphragm radius, the larger the maximum dislocation density is. This is because large diaphragm induces high von Mises effective stress near the diaphragm edge. Thus the plastic shear strain rate in the region is high accordingly.



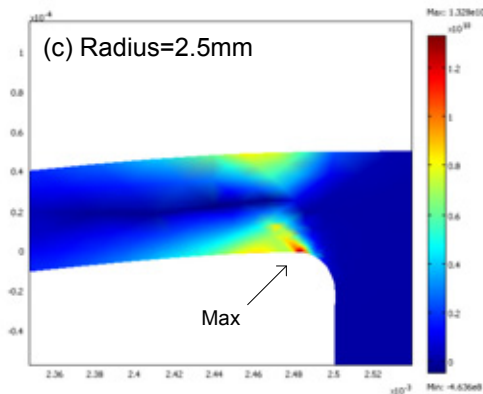


**Figure 7** The dislocation density distribution after annealing at the region near the diaphragm edge (deformed geometry) (a) Radius=1.5mm; (b) Radius=2mm; (c) Radius=2.5mm.

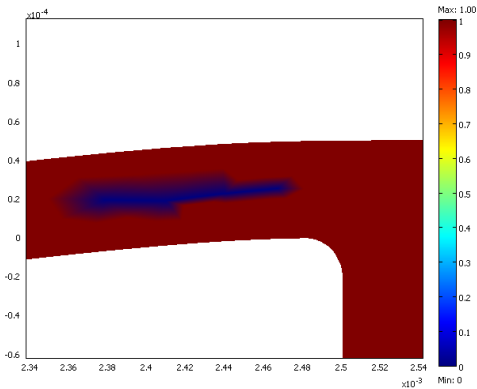


**Figure 8** The deformed geometry at the diaphragm edge (Radius=2.5mm). The positive dislocation density is illustrated by the red color while the negative dislocation density is illustrated by the blue color

The maximum dislocation density for the diaphragm with a radius of 2.5mm is about  $1.32 \times 10^{10} / \text{m}^2$  as shown in figure (c). Since the dislocation density is very high, the dislocations generated on different slip systems begin to interact with each other, thus making the plastic deformation much difficult. The simulated results show that the dislocation density becomes negative at the region close to the middle plane, as illustrated by the blue color in figure 8. In fact, the dislocation density at the blue region should be very close to the initial value. Because the stress near the middle plane is very low, the dislocation multiplication rate could be very low according to equation 3, or equal to zero if  $\tau < \alpha \mu b$ . The negative dislocation density from the

simulation results is caused by the convergence problem of the FEA model due to the highly non-linear material properties. In order to prevent numerical overshoot in the value of dislocation density, a refined mesh at the location with high stress concentration is applied. The absolute value of the dislocation density is used for equation (2) in order to avoid the root of a negative.

## 5.2 Diaphragm displacement

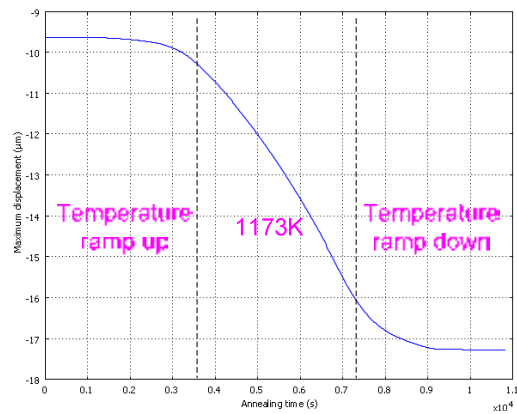


**Figure 9.** The evolution of the maximum displacement with time (radius=1.75mm)

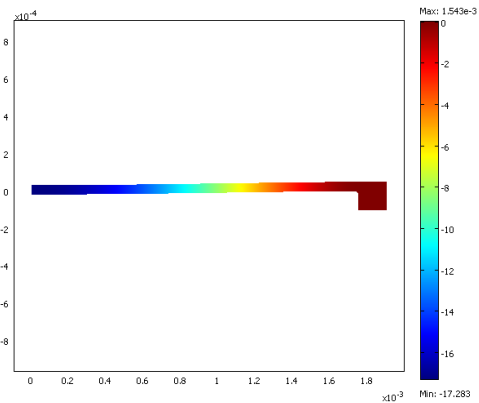


**Figure 10.** The deformation of a silicon diaphragm after annealing (radius=1.75mm)

The main interest in the diaphragm behavior for the micromachined pressure sensor application is the diaphragm deformation. The evolution of the maximum displacement of the diaphragm with a radius of 1.75mm is shown in figure 9. The initial displacement is induced by the atmospheric pressure. The plastic shear strain rate increases with temperature according to

equation (1). Therefore, the creep process is much faster at 1173K (900°C) than that at the temperature ramp. The deformation of the silicon diaphragm after annealing is shown in figure 10. The maximum displacement is 17.28 $\mu$ m at the centre of the diaphragm.

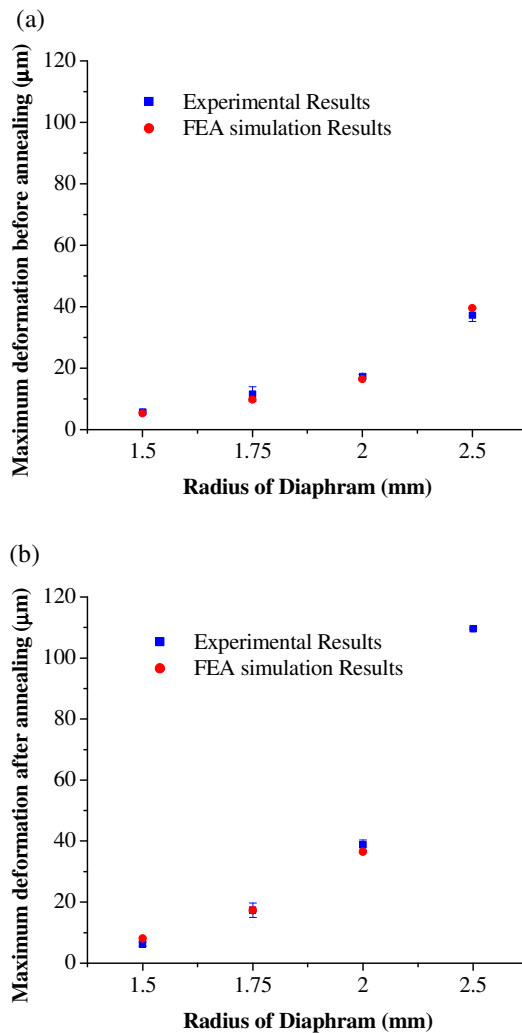


**Figure 11.** The comparisons of experimental data and model prediction for the diaphragm displacement (a) before annealing (b) after annealing.

Figure 11 illustrates the comparisons between the experimental displacement data and the prediction from the AH model for various diaphragm radius. It can be seen that the simulated deformation match well with the measured data for the diaphragms with a radius of 1.5mm, 1.75mm and 2mm. Because the effect

of the dislocations interaction on the plastic deformation is not included in the model, the predicted maximum displacement of 318.19 $\mu$ m is much larger than the measure data of 110  $\mu$ m for the diaphragm with a radius of 2.5mm.

## 6. Conclusion

A finite element model is presented in this paper to predict the mechanical behavior of micromachined silicon diaphragms at 900°C in the initial deformation stage. The model is based on the constitutive equations proposed by Alexander and Hassen. This model uses two PDE general form modes coupled with the stress-strain application mode. The plastic strain is determined by the plastic shear strain rate, which is related to the evolution of the dislocation density. The dislocation density distribution and the diaphragm displacement are obtained for each diaphragm size. The predicted results are in agreement with the measured data for the diaphragms with a radius in the range of 1.5mm to 2mm. The model is not valid for the diaphragm with a radius of 2.5mm since the generated dislocation density is very high, and the slip resistance should be considered. Current experiment condition allows checking the simulated displacement by the experiment. However, the creep deformation is dependent on the velocity and the density of the moving dislocations. Therefore, it is necessary to check the dislocation density in the diaphragm after the samples were exposed to annealing. At the same time, the model assumes that the material is homogenous and the deformation is uniform. Therefore, the model could be improved if the plastic deformation on each slip system is concerned.

## 7. References

1. S. Beeby, G. Ensell, M Kraft and N White, *MEMS Mechanical Sensors*, Artech House, Boston, (2004)
2. Seyed M. Allameh, *Silicon-Based Microelectronmechanical Systems (Si-MEMS)* in: W. O. Soboyejo and T. S. Srivatsan, *Advanced structural materials: properties, design optimization, and applications*. CRC Press, Taylor & Francis Group (2006)

3. H. Alexander and P. Haasen, Dislocation and plastic flow in the diamond structure, *Solid State Phys*, Volume 22, Pages 27–158 (1968)
4. M. M. Myshlyaev, V. I. Nikitenko, V. I. Nesterenko, Dislocation structure and macroscopic characteristics of plastic deformation at creep of silicon crystals, *physica status solidi*, Volume 36, Pages 89-95 (1969)
5. Moon H-S, Anand L, Spearing SM. A constitutive model for the mechanical behavior of single crystal silicon at elevated temperatures. In: *Mat Res Soc Symp Proc* 687, Paper B9.6, (2002)
6. Cacho, F.Orain, S.Cailletaud, G.Jaouen, H., A constitutive single crystal model for the silicon mechanical behavior: applications to the stress induced by silicided lines and STI in MOS technologies, *Microelectronics Reliability*, Volume 47, Pages 161-167 (2007)
7. Lohonka, R., G. Vanderschaeve, et al, Modelling of the plastic behaviour of III-V compound semiconductors during compressive tests, *Materials Science and Engineering A*, Volume 337, Issues 1-2, Pages 50-58 (2002)
8. J. Ren, D. Cheneler, Mike Ward and Peter Kinnell, The Mechanical Behaviours of Circular SCS Diaphragm for Micromachined Capacitive Pressure Sensor. *Advances in Science and Technology*, Volume 54, Pages 422-427 (2008)
9. Imai, M. and K. Sumino (1983). In situ X-ray topographic study of the dislocation mobility in high-purity and impurity-doped silicon crystals. *Philosophical Magazine A*, Volume 47, Pages 599-621 (2008)

## 8. Acknowledgements

The author would like to thank Dr Peter Hartley for the helpful discussion about the continuum mechanics. Thanks to Dr Wen Zhang, Rune Westin and Remi Magnard at COMSOL Ltd for their technical support.